Biological systems, imaging techniques

Maxwell-Wagner relaxation

Valerică Raicu
Departments of Physics and Biological Sciences
University of Wisconsin-Milwaukee
http://www.uwm.edu/Dept/Physics/Raicu/

Novel Applications of Broadband Dielectric Spectroscopy, Rome, August, 2009

Phenomenological analysis of interfacial polarization

Free charge movement in electric field

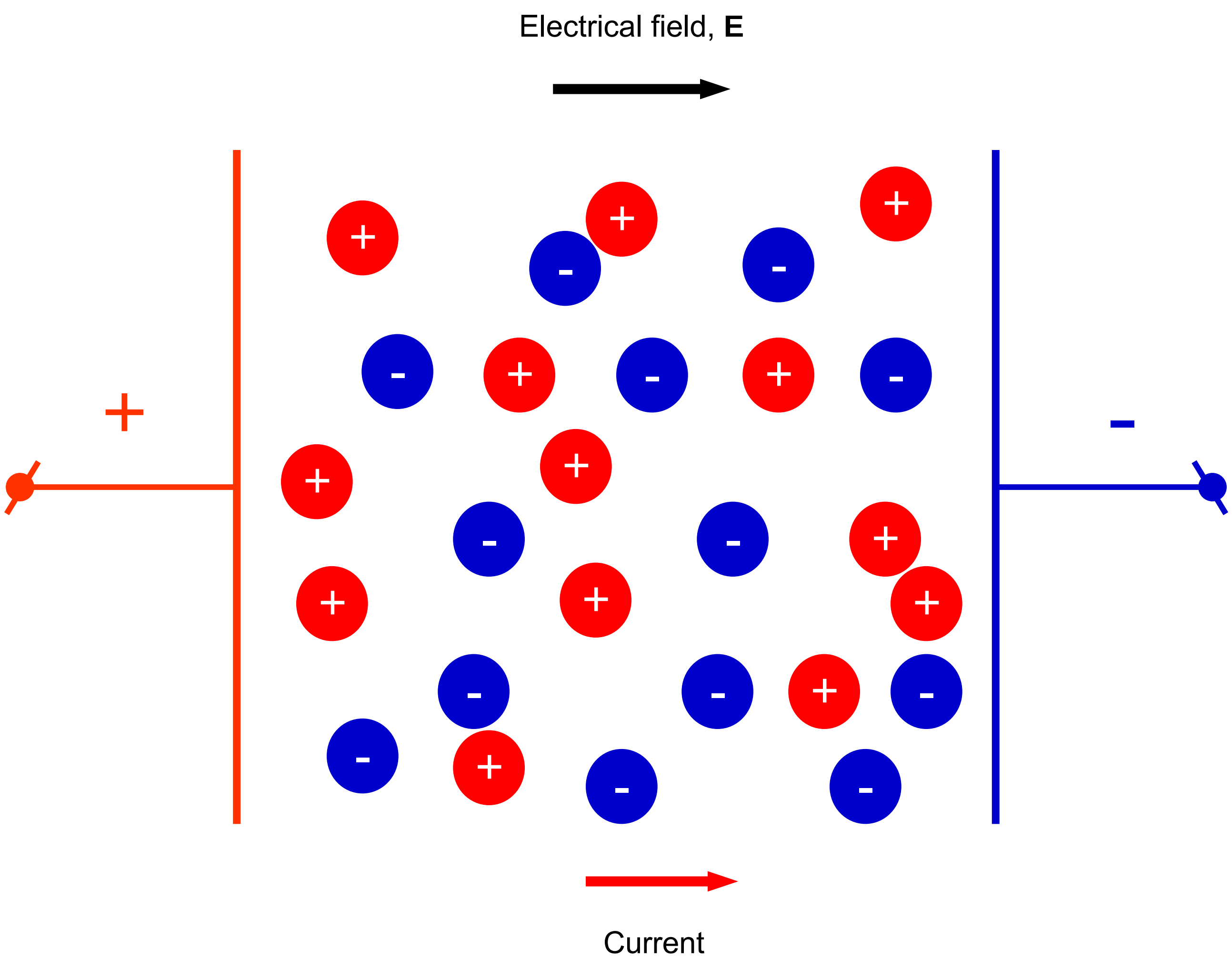

Interfacial polarization

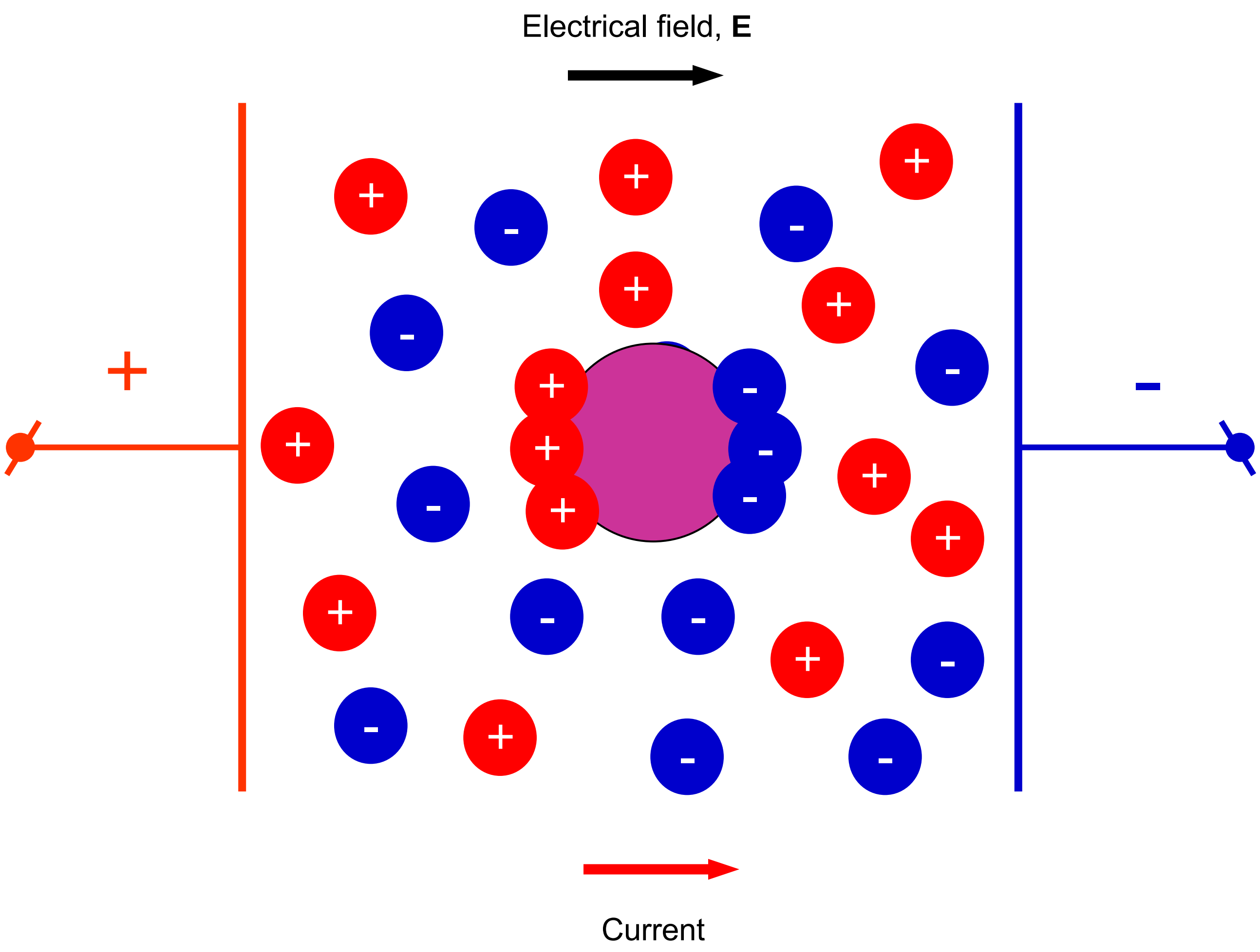

Different types of dipoles, same formalism

Permanent

(Ex: H_2O)

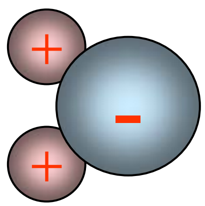

Induced

(by interfacial polarization)

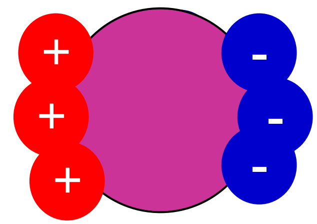

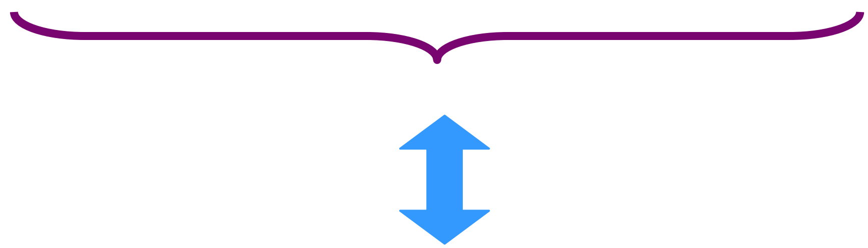

Dipole model

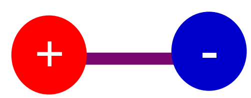

Response of dipoles to E field

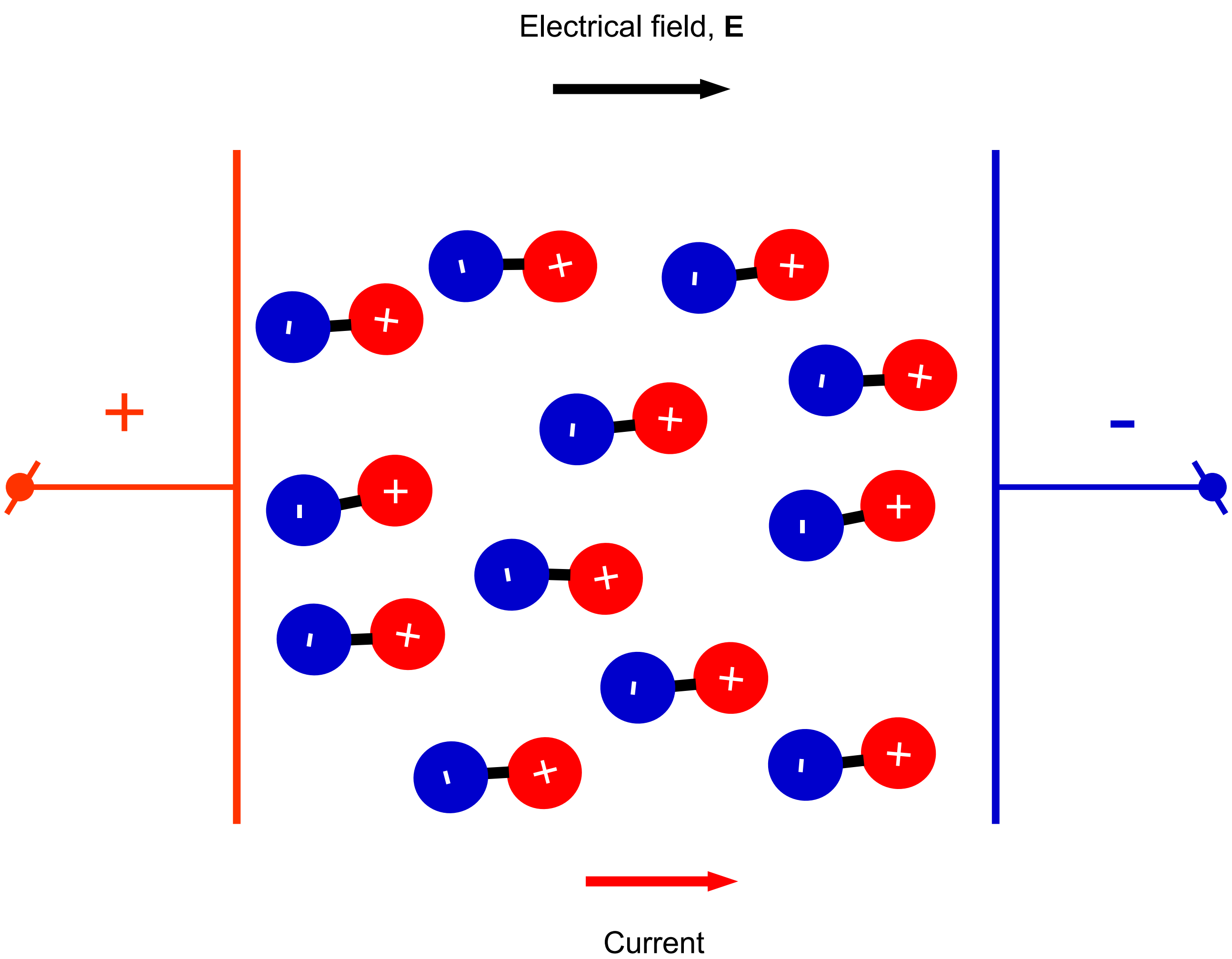

Dielectric dispersion

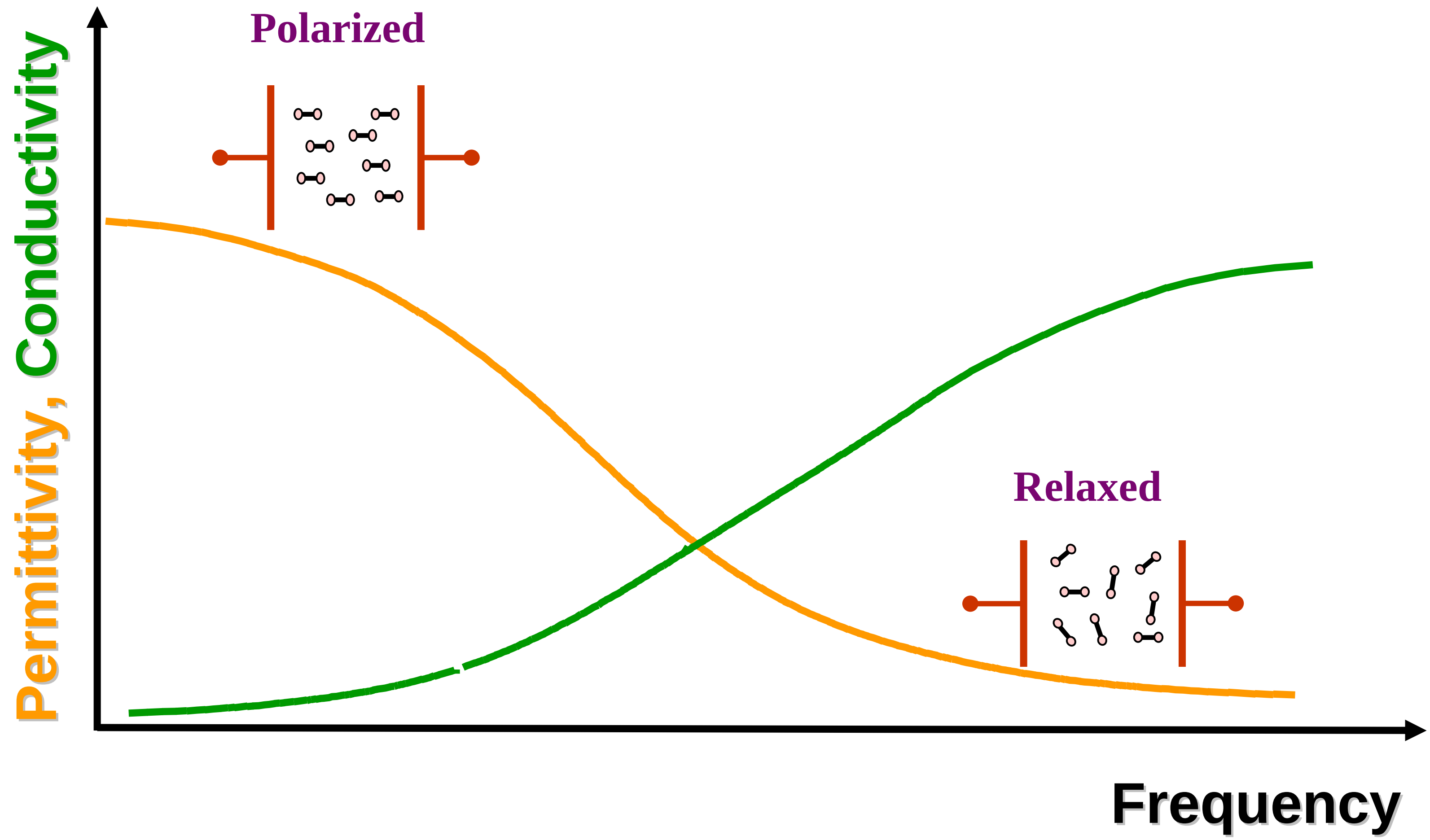

Complex permittivity

Definition:

$$\varepsilon^* \equiv \varepsilon + i\frac{\sigma}{2\pi f}$$

Debye dispersion function in complex form:

$$\varepsilon^* = \varepsilon_h + \frac{\delta\varepsilon}{1 + i\, f / f_c} + i\frac{\sigma_l}{2\pi f}$$

Debye dispersion function

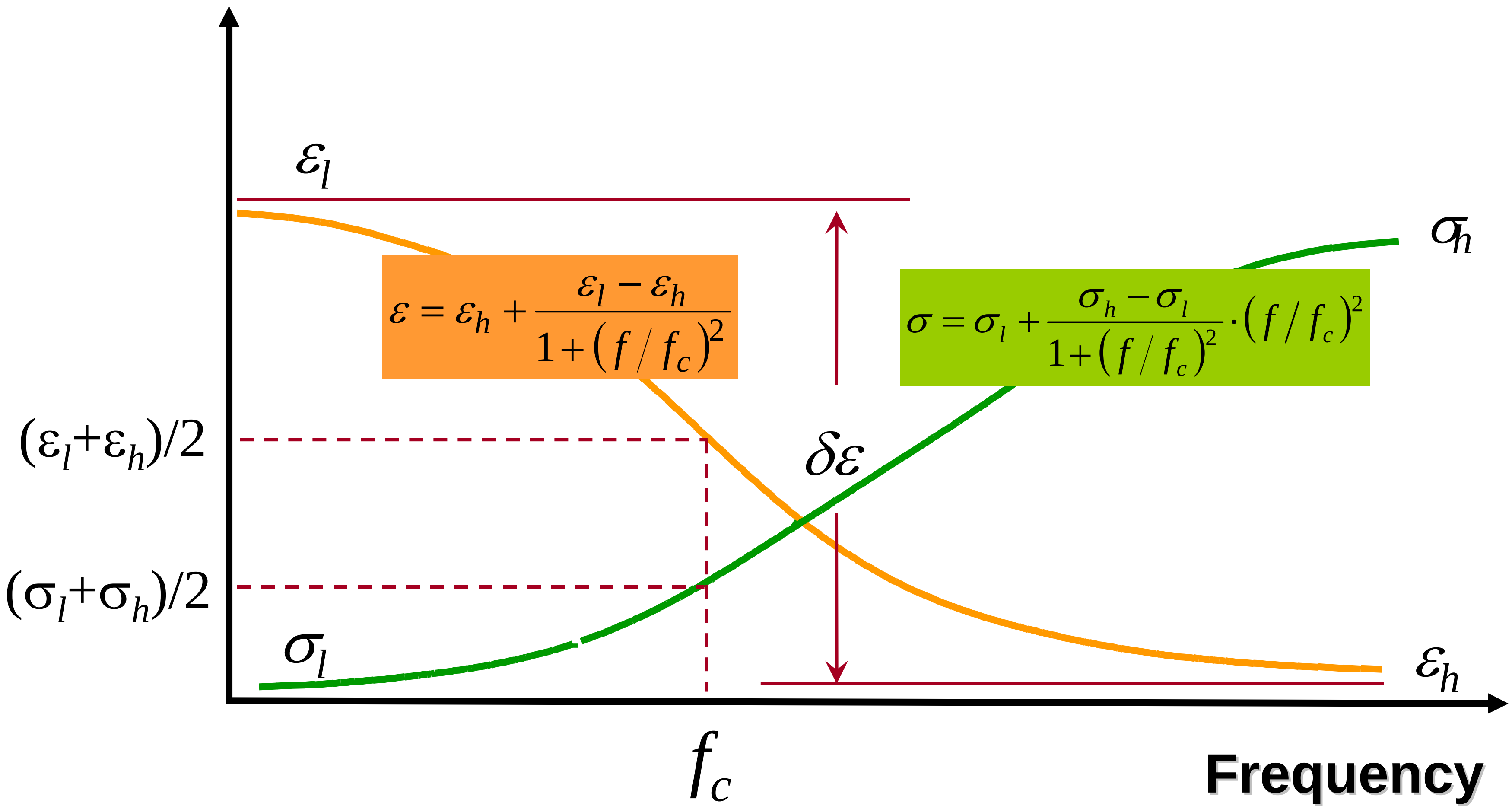

A general dispersion function (GDF)

$$\varepsilon^* = \varepsilon_h + \frac{\Delta}{[(i\,f/f_c)^{\alpha} + (i\,f/f_c)^{1-\beta}]^{\gamma}} - i\frac{\sigma_l}{2\pi\varepsilon_o f}$$

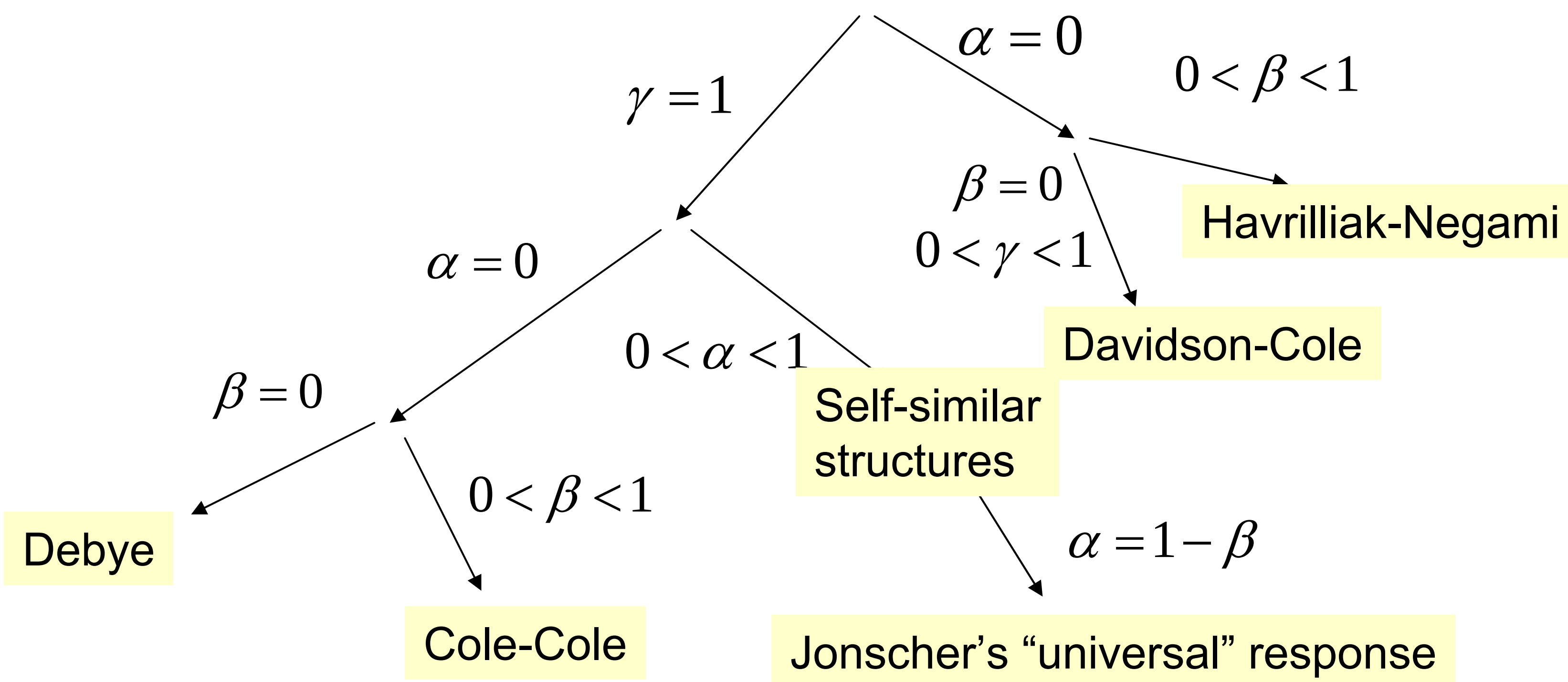

V. Raicu, *Phys. Rev. E* 60 (1999) 4677-4680

GDF includes both tissue and suspension responses

$$\varepsilon_s^* = \varepsilon_h + \frac{\Delta}{[(i\,f/f_c)^{\alpha} + (i\,f/f_c)^{1-\beta}]^{\gamma}} - i\frac{\sigma_l}{2\pi\varepsilon_o f}$$

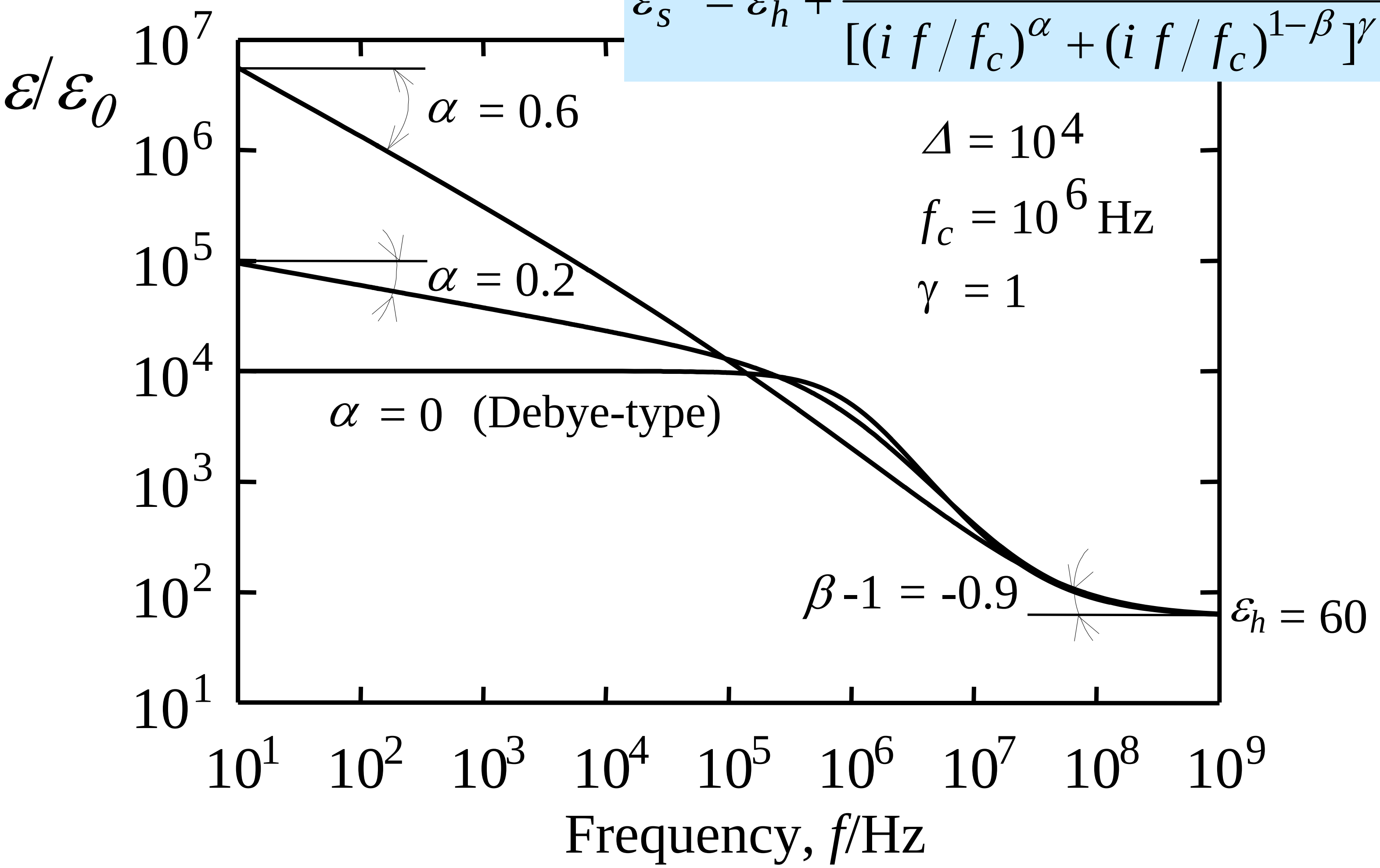

Maxwell-Wagner model of interfacial polarization

Interfacial polarization (Maxwell-Wagner relaxation)

To calculate the electric potential at an external point P, due to ***n*** particles of permittivity ε_p, one assumes that the particles in the large sphere are so far away from P, that they appear to be at the same distance, r, from P.

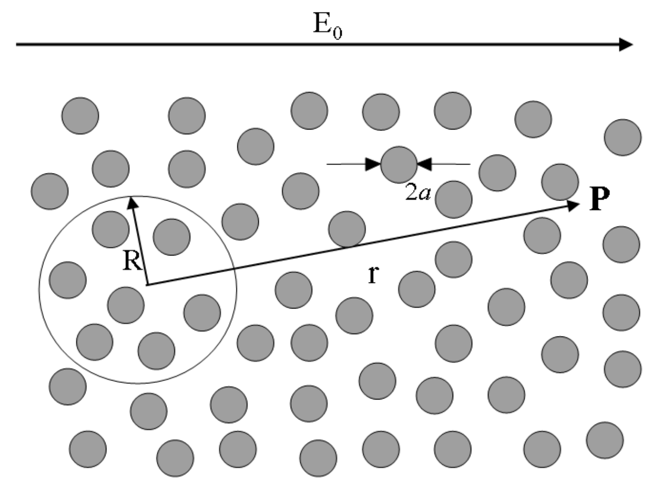

The result is found in standard electrodynamics textbooks (e.g., Jackson):

$$\Phi(r,\theta) = -E_0 r \cdot \cos\theta + n\frac{a^3}{r^2} \cdot \frac{\varepsilon_p^* - \varepsilon_e^*}{\varepsilon_p^* + 2\varepsilon_e^*} E_0 \cos\theta \qquad (\text{for } r >> \text{R})$$

Interfacial polarization (Maxwell-Wagner relaxation)

The potential due to the large sphere, assumed to be homogeneous and of permittivity ε, *is*:

$$\Phi(r,\theta) = -E_0 r \cdot \cos\theta + \frac{R^3}{r^2} \cdot \frac{\varepsilon^* - \varepsilon_e^*}{\varepsilon^* + 2\varepsilon_e^*} E_0 \cos\theta$$

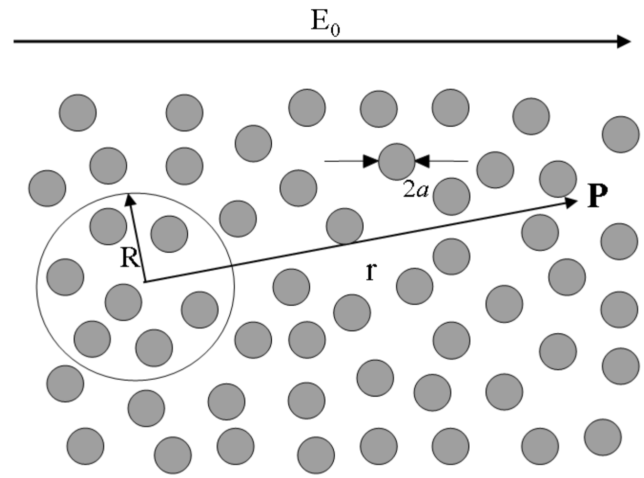

An equation for permittivity is obtained assuming equality of the two potentials:

$$\frac{\varepsilon^* - \varepsilon_e^*}{\varepsilon^* + 2\varepsilon_e^*} = p \cdot \frac{\varepsilon_p{}^* - \varepsilon_e^*}{\varepsilon_p{}^* + 2\varepsilon_e^*} \quad \text{with} \quad p = n\frac{a^3}{R^3}$$

This is known as the Maxwell-Wagner equation.

S. Takashima, *Electrical properties of biopolymers and cell membranes*, Adam Hilger, 1989

V. Raicu and A. Popescu, *Integrated Molecular and Cellular Biophysics*, Springer, 2008

Equivalent permittivity of suspensions of shelled spheres

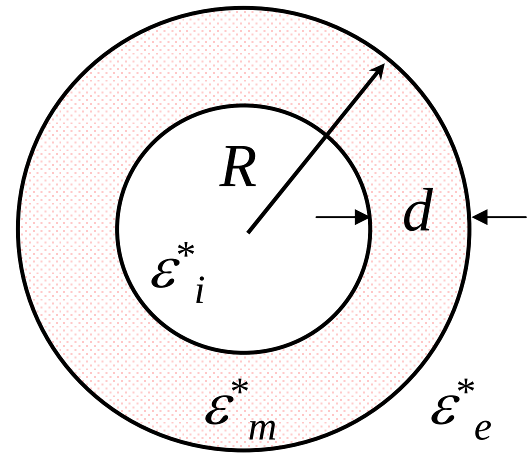

Miles and Robertson [Phys Rev (1932), **40:** 583] calculated the potential outside shelled spheres suspended in a medium of permittivity ε_e,

$$\Phi(r,\theta)=-E_0 r\cdot\cos\theta+n\frac{R^3}{r^2}\cdot\frac{(\varepsilon_m^*-\varepsilon_e^*)(\varepsilon_i^*+2\varepsilon_m^*)+(\varepsilon_i^*-\varepsilon_m^*)(\varepsilon_e^*+2\varepsilon_m^*)v}{(\varepsilon_m^*+2\varepsilon_e^*)(\varepsilon_i^*+2\varepsilon_m^*)+2(\varepsilon_i^*-\varepsilon_m^*)(\varepsilon_e^*-\varepsilon_m^*)v}E_0\cos\theta$$

The potential due to a spherical suspension of such particles of equivalent ε is

$$\Phi(r,\theta)=-E_0 r\cdot\cos\theta+\frac{\rho^3}{r^2}\cdot\frac{(\varepsilon^*-\varepsilon_e^*)}{(\varepsilon^*+2\varepsilon_e^*)}E_0\cos\theta$$

The equation for permittivity, obtained from equality of the two potentials, is then

$$\frac{\varepsilon^*-\varepsilon_e^*}{\varepsilon^*+2\varepsilon_e^*}=p\cdot\frac{(\varepsilon_m^*-\varepsilon_e^*)(\varepsilon_i^*+2\varepsilon_m^*)+(\varepsilon_i^*-\varepsilon_m^*)(\varepsilon_e^*+2\varepsilon_m^*)v}{(\varepsilon_m^*+2\varepsilon_e^*)(\varepsilon_i^*+2\varepsilon_m^*)+2(\varepsilon_i^*-\varepsilon_m^*)(\varepsilon_e^*-\varepsilon_m^*)v} \quad \text{with} \quad p=nR^3/\rho^3 \quad \text{and} \quad v=(R-d)^3/R^3$$

This equation is sometimes improperly attributed to Pauly and Schwan.

Approximations to the single shell model

For single-shelled particles, only one dispersion is usually important – the one due to the polarization at the interface between the suspending medium and cell membrane.

Pauly and Schwan have considered the very reasonable approximations,

$$\frac{\sigma_m}{\sigma_e}, \frac{\sigma_m}{\sigma_i}, \frac{d}{R} << 1,$$

from which they obtained the parameters corresponding to **a single Debye equation**:

$$\delta\varepsilon \equiv \varepsilon_l - \varepsilon_h = \frac{9p}{(2+p)^2}\frac{RC_m}{\varepsilon_0} \qquad \tau \equiv \frac{1}{2\pi f_c} = RC_m\left(\frac{1}{\sigma_i} + \frac{1-p}{2+p}\frac{1}{\sigma_a}\right) \qquad \sigma_l = \sigma_e \frac{2(1-p)}{2+p}$$

where $C_m = \frac{\text{membrane capacitance}}{\text{surface area}} \equiv \frac{\varepsilon_m}{d}$ is the specific membrane capacitance

and $\varepsilon_0 = 8.854 \times 10^{-12}$ F/m is the permittivity of the free space.

S. Takashima, *Electrical properties of biopolymers and cell membranes*, Adam Hilger, 1989
V. Raicu and A. Popescu, *Integrated Molecular and Cellular Biophysics*, Springer, 2008

Multiple membranes: decomposition into sub-dispersions

- Daenzer H (Ergenbnisse der Biophysikalischen Forschung, ed E.B. Rajewsky, Leipzig: Georg Thieme, 1938, pp193-231), and later Pauly and Schwan (*Z. Naturforsch.* 14b, 1959, 125) have found that the complex permittivity expression for shelled spheres is exactly decomposable into two terms of a Debye type, corresponding to the two interfaces of the particles.

- Fricke (*J. Phys. Chem.*, 59, 1955, 168) has generalized the model to include multi-shelled particles, and obtained an equivalent admittance if the form of a continued fraction.

- Irimajiri, Hanai, and Inouye (*J. Theor. Biol.*, 78, 1979, 251-269) have succeeded in decomposing the dielectric function for multi-shelled particle suspensions into a sum of sub-dispersions whose total number equaled the number of cell interfaces.

Supra-cellular architecture

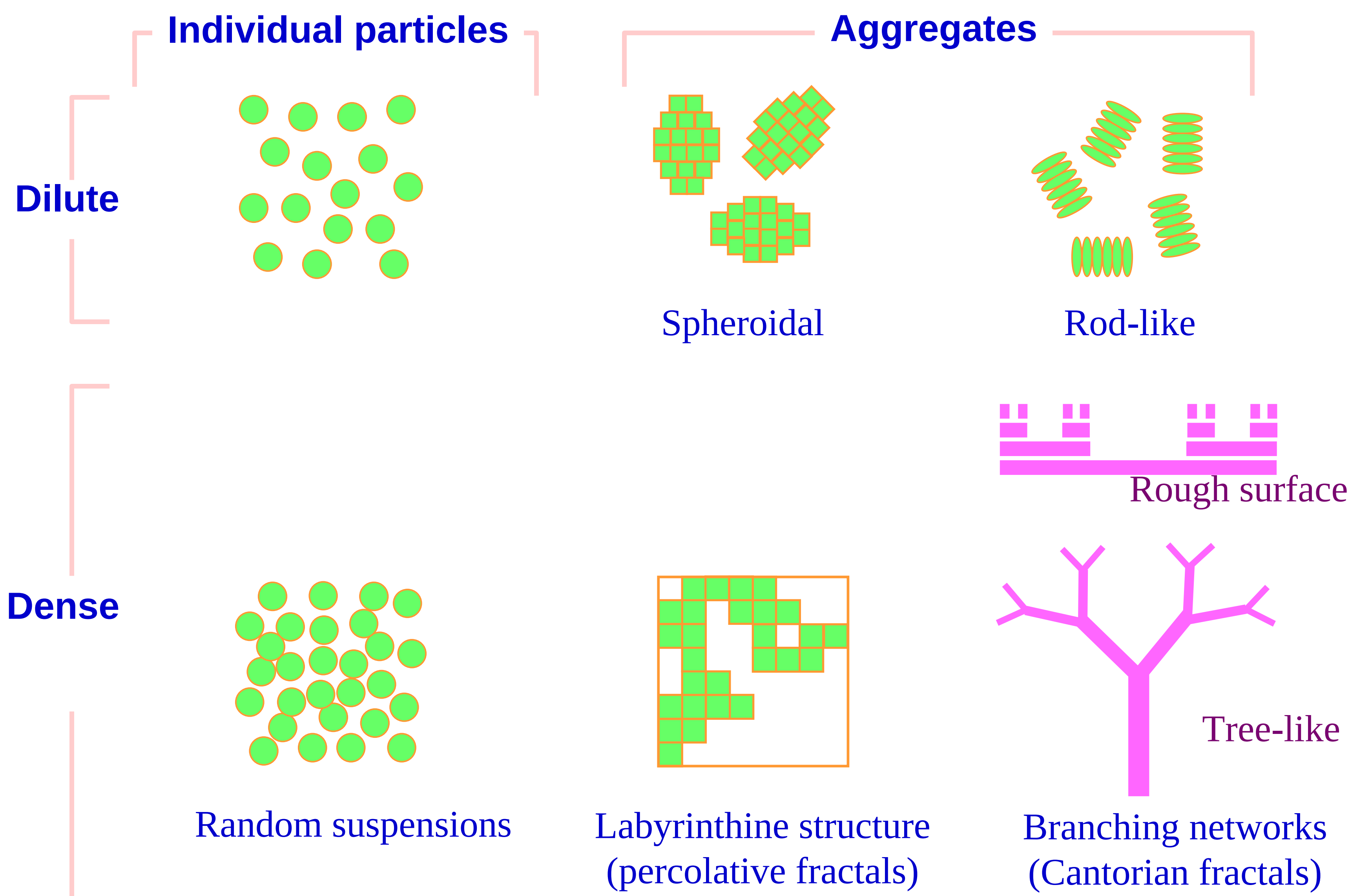

Effective Medium Theory (EMT)

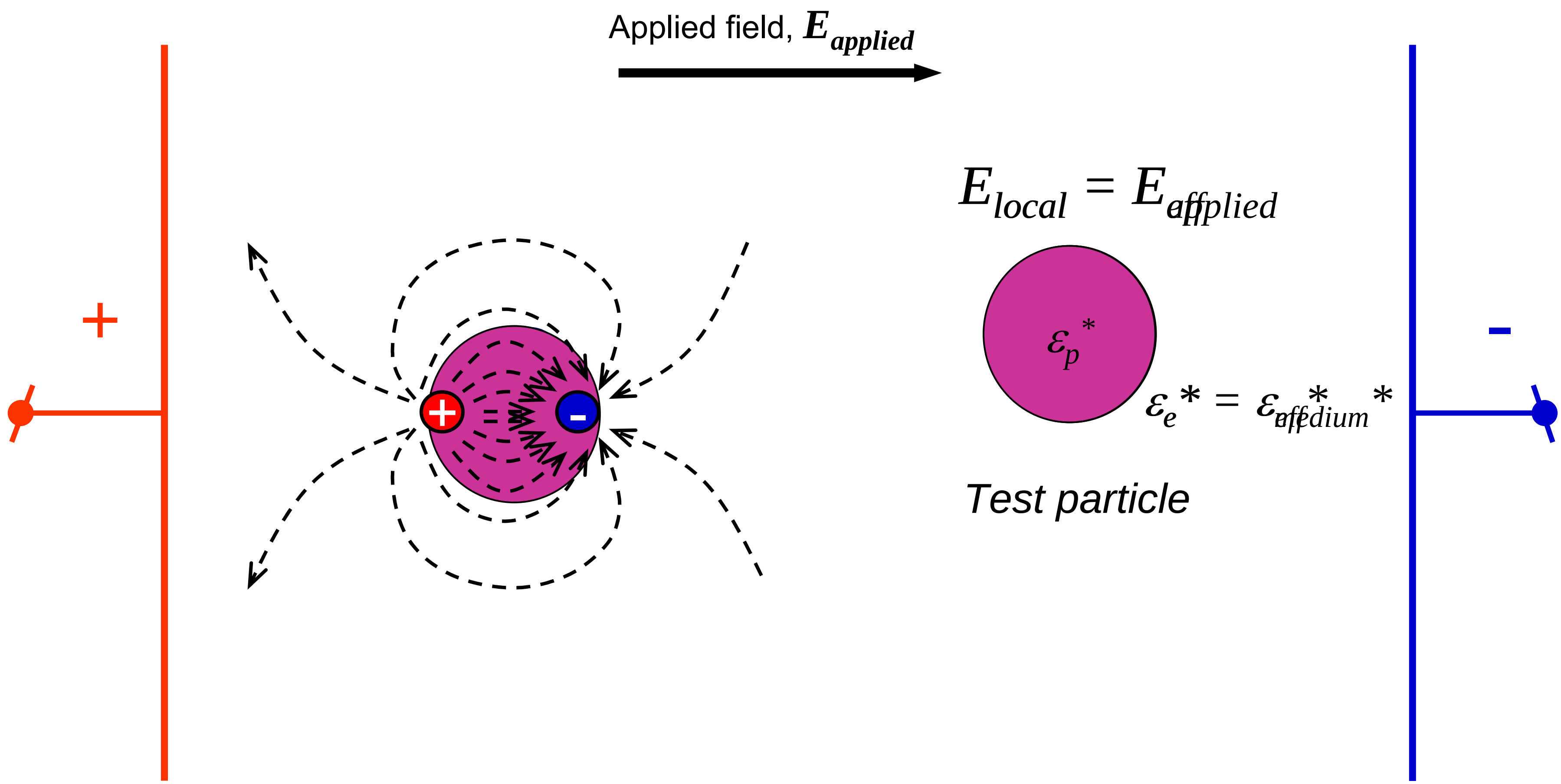

- EMT takes into account contributions of other cells' far-field to the local field
- Introduced by Brugemann and further developed by Hanai (see Takashima's book)

EMT with Dipole-Dipole Interactions (EMT-DDI)

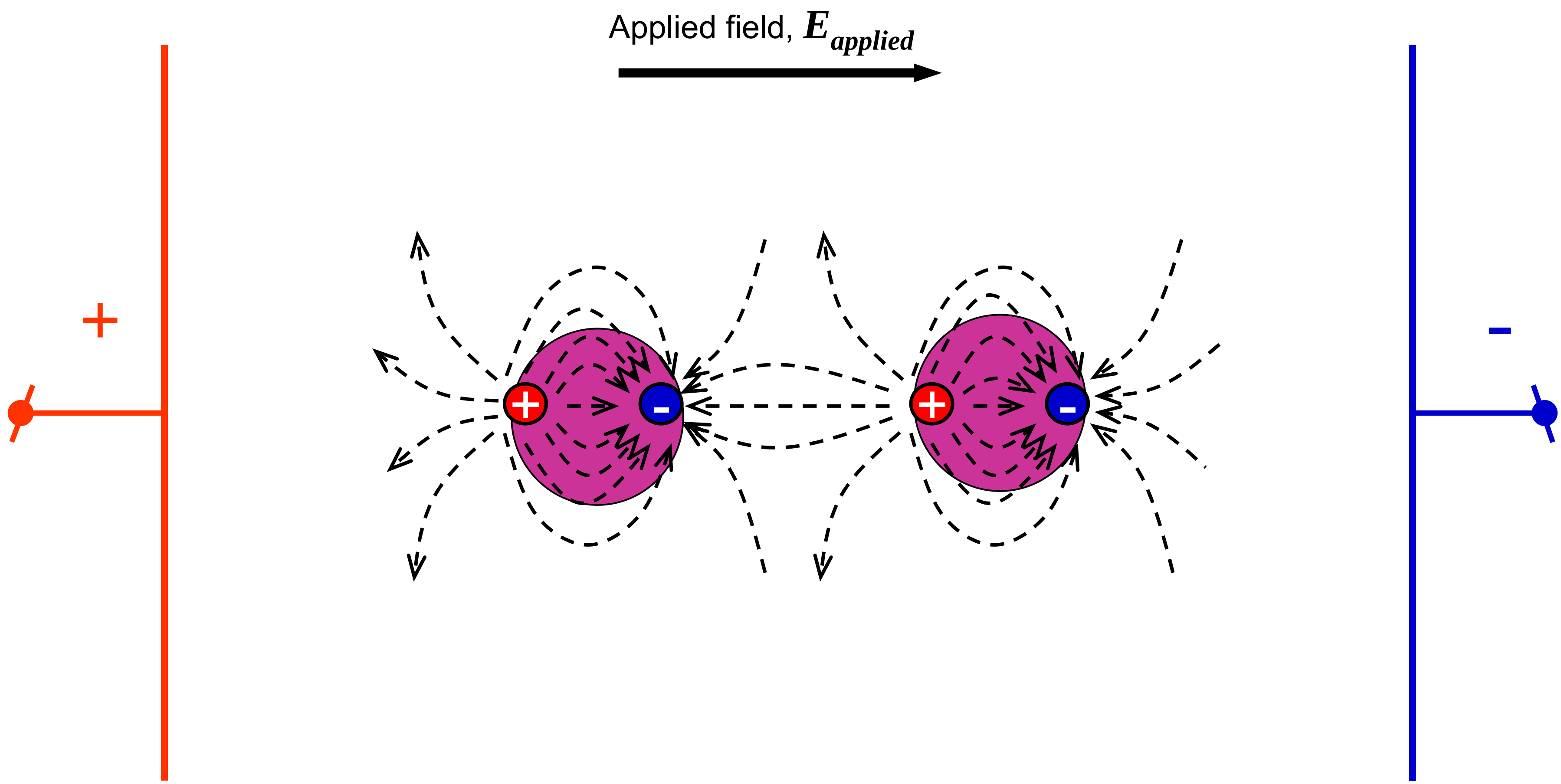

- EMT-DDI takes into account contributions of cells to the local field
- Higher order multipoles should be also considered → This is very difficult !!

V. Raicu, T. Saibara, H. Enzan and A. Irimajiri, *Bioelectrochem. Bioenerg.,* **47** (1998) 333-342

Applications

Standard two-electrode systems for dielectric measurements

Open-ended coaxial probe

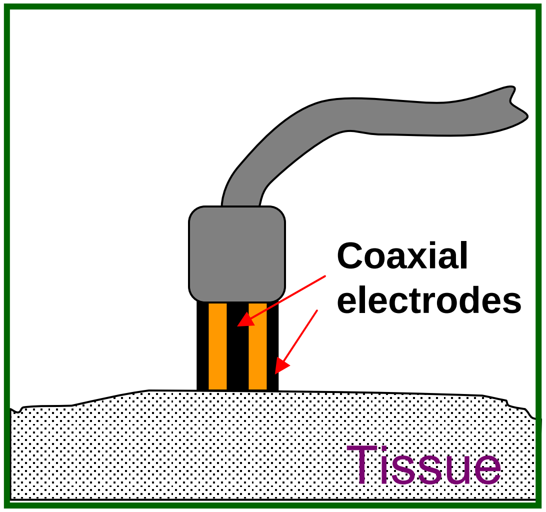

Raicu, V., *Measurement Science & Technology*, 1995. **6**(4): 410-414

Parallel-plate capacitor

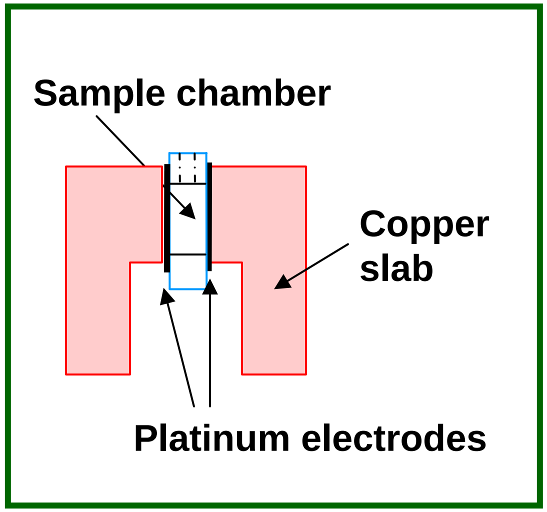

Schwan, H.P., In: *Physical Techniques in Biological Research*, W.L. Nastuk, Editor. 1963, Academic Press: New York, p. 323-407

Pin-like electrodes

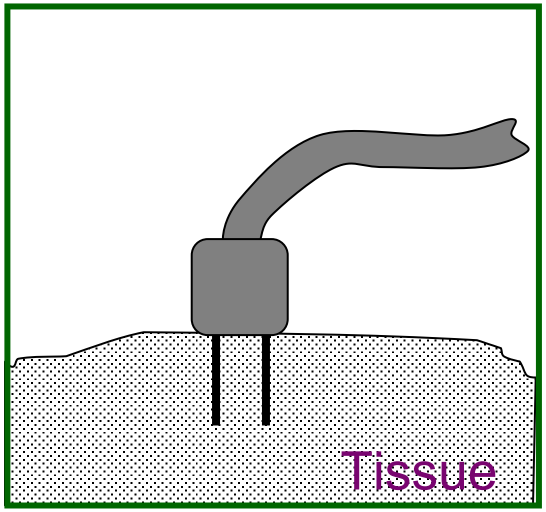

Stoneman et al, *J. Noncrystalline Solids*, in press

Dilute, random suspensions of cells

Debye-type dispersion

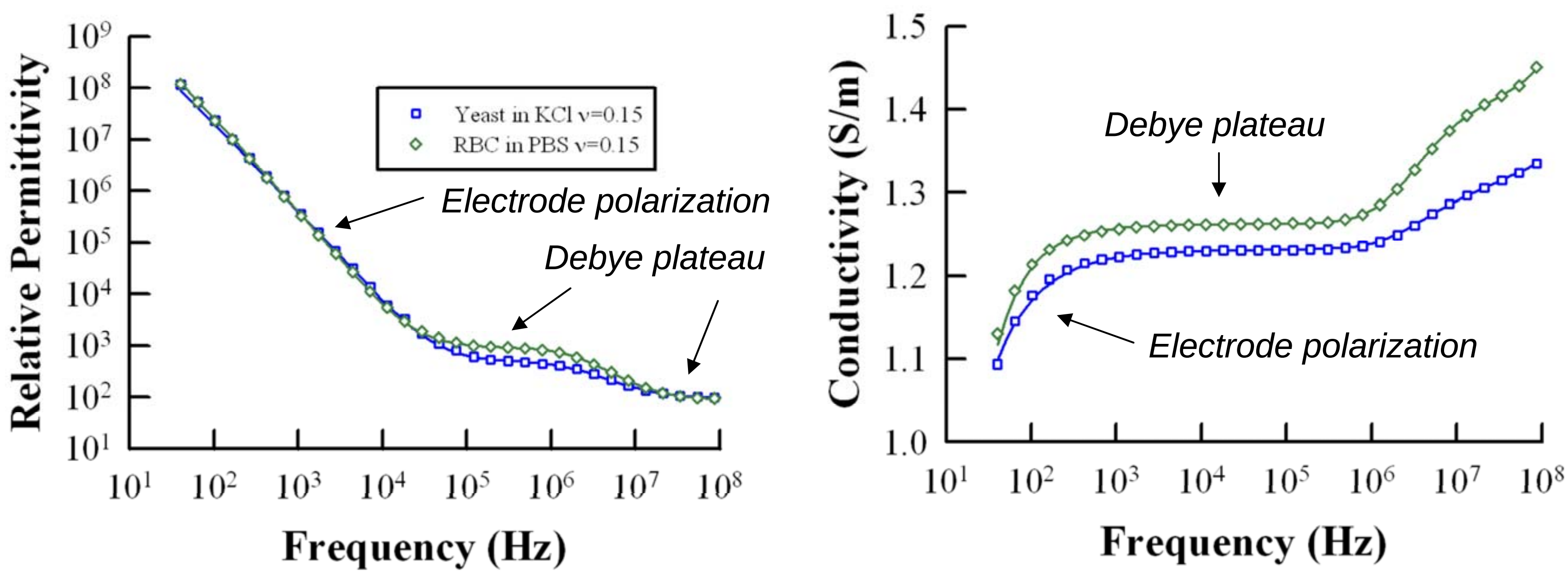

- Follow Maxwell-Wagner model → **particles subjected to uniform far-field**
- Particle shape introduces some quantitative but not qualitative differences

Dilute, random suspensions of cells

Extraction of cellular parameters

Specific plasma membrane capacitance is easily determined:

- Erythrocyte ghosts: 0.72 μF/cm^2 [K. Asami, T. Takahashi, and S. Takashima, 1989, *Biochim. Biophys. Acta*, 1010: 49-55]
- Plant protoplasts: 0.6-0.7 μF/cm^2 [Asami and Yamaguchi, 1992, *Biophys. J.*, 63: 1493-1499]

→ Membrane thickness ~3-4 nm (membrane thickness determined using dielectric spectroscopy by Fricke, before the electron-microscope era).

Electrical properties of other cell phases have also been also determined

[F. Bordi, C. Cametti, and T. Gili, 2002, J. Non-Crystalline Solids 305: 278–284]

[Y. Polevaya, I. Ermolina, M. Schlesinger, B-Z. Ginzburg, Y. Feldman, 1999, *Biochim. Biophys. Acta* 1419: 257-271]

[V. Raicu, G. Raicu and G. Turcu, 1996, *Biochim. Biophys. Acta*, 1274: 143-148]

Dilute, random suspensions of cells

Membrane permeabilization by surfactants

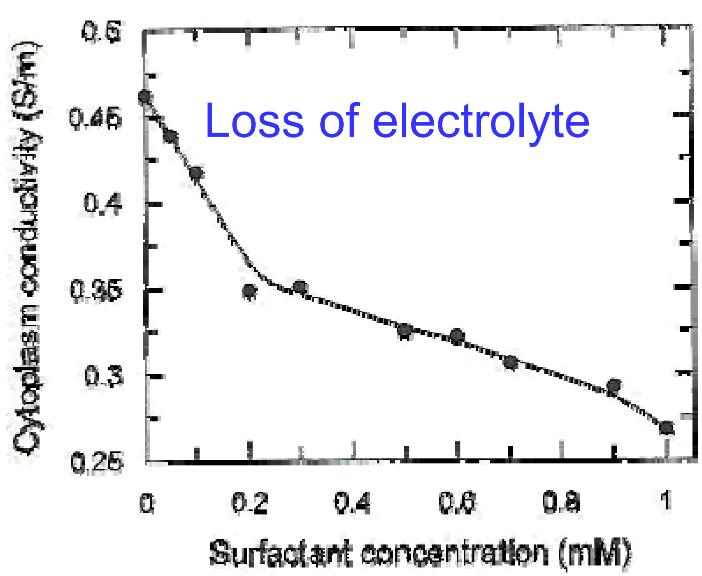

Fig. 3. Electrical conductivity of cytoplasm versus CTAB concentration.

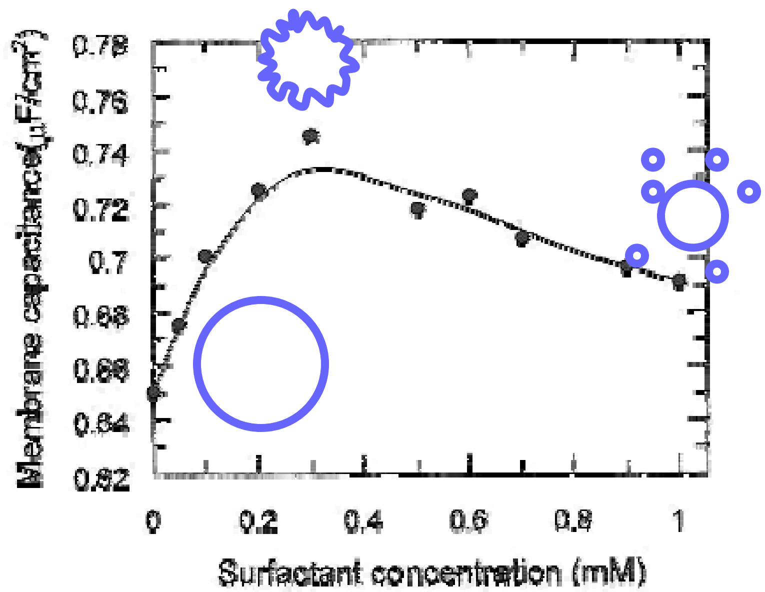

Fig. 4. The dependence of the plasma membrane specific capacitance on CTAB concentration.

V. Raicu, C. Gusbeth, G. Raicu, D. Anghel, G. Turcu, 1998, *Biochim. Biophys. Acta,* **1379:** 7-15

UNIVERSITY of WISCONSIN UWMILWAUKEE

Dielectric modeling of rat liver

Maxwell-Wagner theory (dilute suspension)

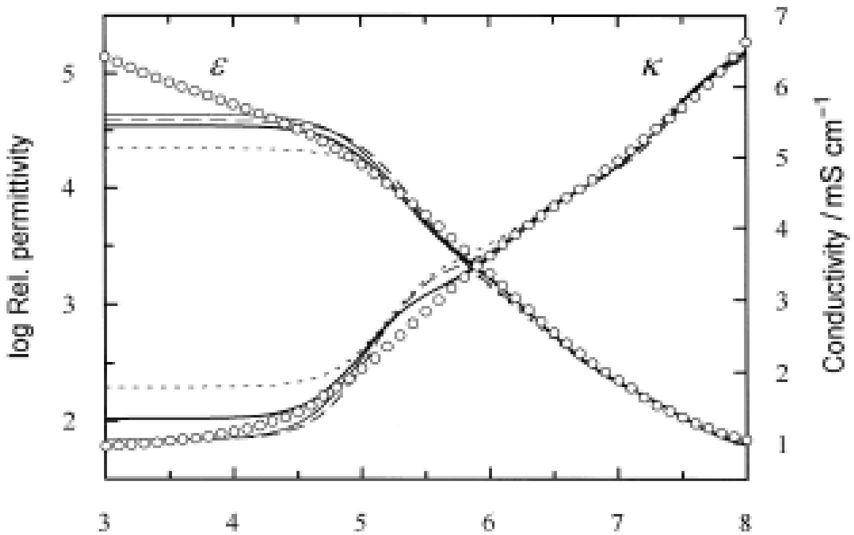

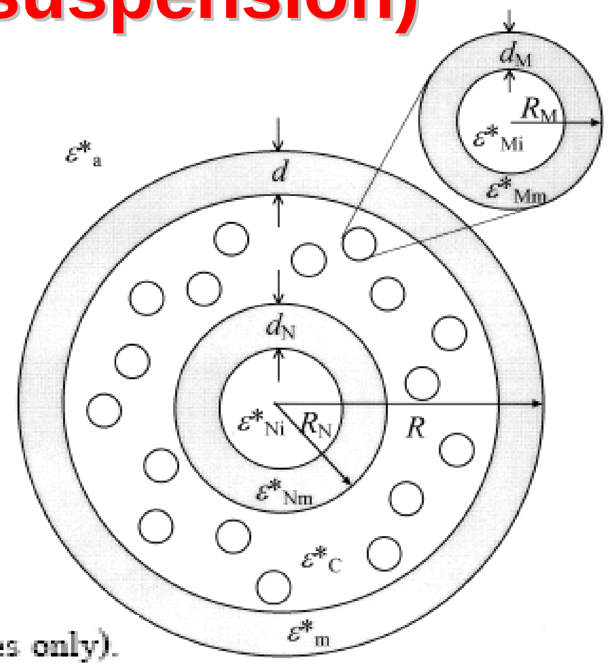

Case 1: Extracellular fluid is blood, $\Phi = 0.719$ (corresponds to hepatocytes only).
Case 2: Extracellular fluid is blood, $\Phi = 0.774$ (includes nonhepatocytes).
Case 3: Homogeneous fluid having $\kappa_a = 6.48$ mS/cm, $\Phi = 0.774$.
Case 4: Cell-free plasma having $\kappa_a = 12$ mS/cm, $\Phi = 0.774$.

- Although all cellular and subcellular components were taken into account, the fit was rather poor.
- Cell volume fraction is high in liver (in excess of 70 %). Maxwell-Wagner approximations break down.

V. Raicu, T. Saibara, H. Enzan and A. Irimajiri, *Bioelectrochem. Bioenerg.*, **47** (1998) 333-342

Dielectric modeling of rat liver

EMT for random concentrated suspensions

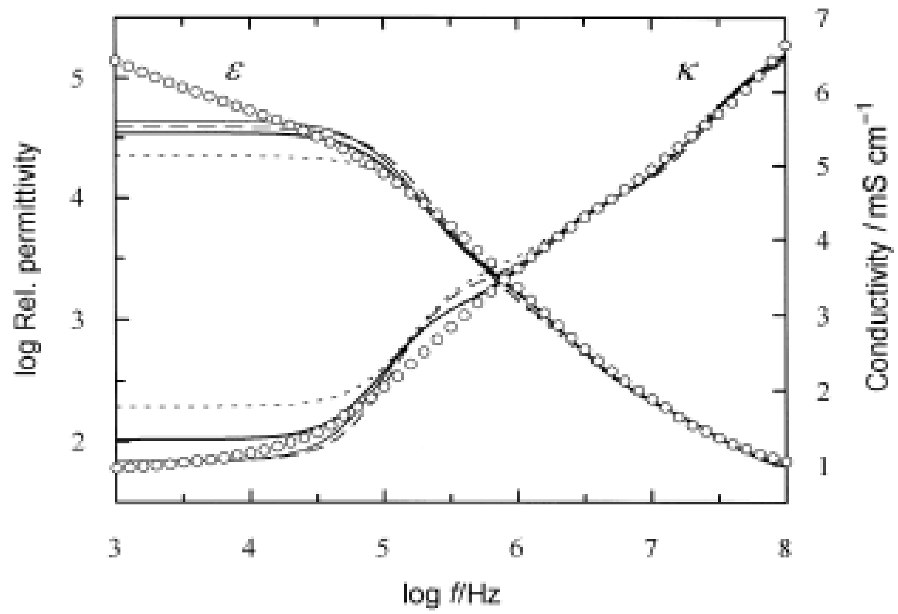

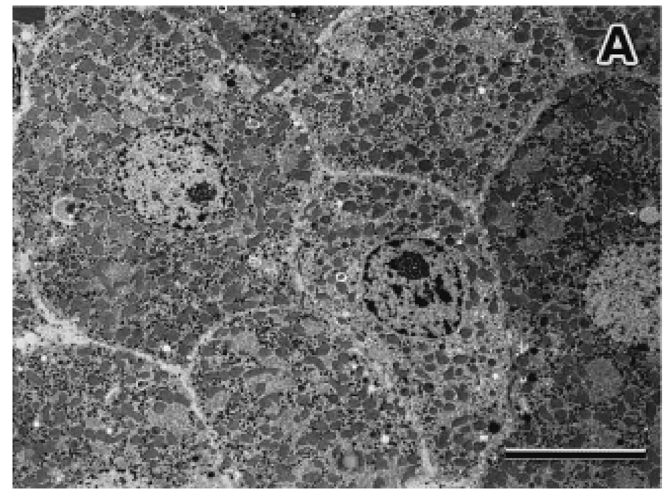

Case 1: Extracellular fluid is blood, $\Phi = 0.719$ (corresponds to hepatocytes only).
Case 2: Extracellular fluid is blood, $\Phi = 0.774$ (includes nonhepatocytes).
Case 3: Homogeneous fluid having $\kappa_a = 6.48$ mS/cm, $\Phi = 0.774$.
Case 4: Cell-free plasma having $\kappa_a = 12$ mS/cm, $\Phi = 0.774$.

- The improvements brought about by EMT were only marginal and the electrical parameters of cells were incorrect (compared to known values for many cell types).
- One reason is that the cells are not randomly dispersed.

V. Raicu, T. Saibara, H. Enzan and A. Irimajiri, *Bioelectrochem. Bioenerg.*, **47** (1998) 333-342

Dielectric modeling of rat liver

Analysis using EMT-DDI

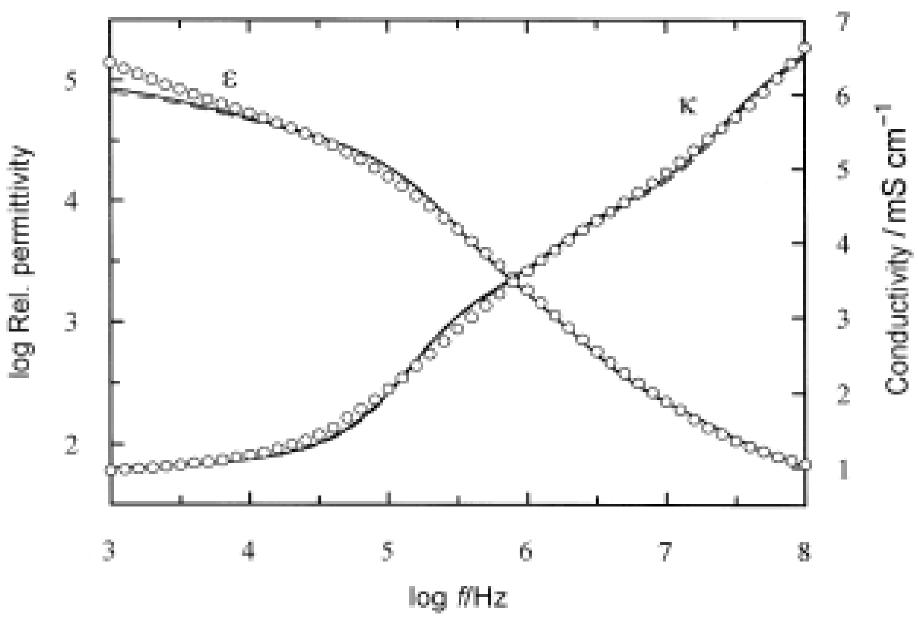

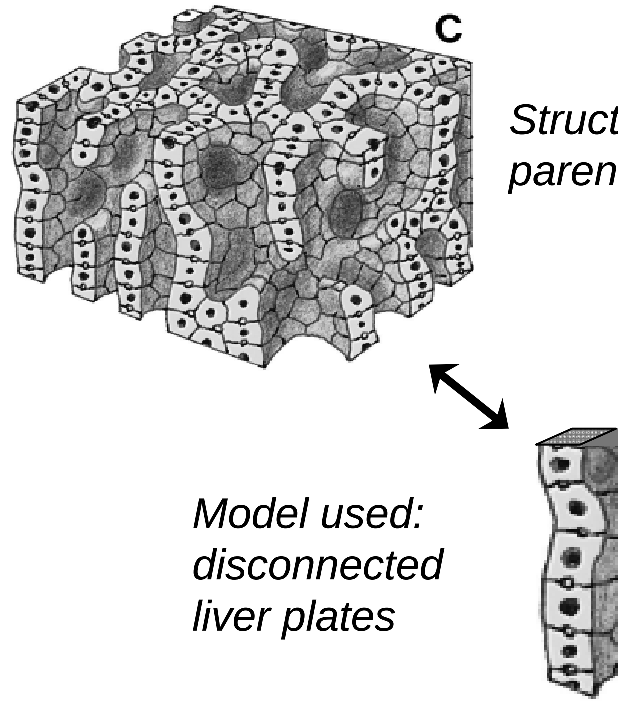

Structure of liver parenchyma

Model used: disconnected liver plates

➢ The improvement was significant and electrical parameters of cells were correct (compared to known values for many cell types).
➢ Yet, the theory failed to account for the absence of Debye-like plateau at low frequencies (perhaps because of the disconnected geometry of the model)

V. Raicu, T. Saibara, H. Enzan and A. Irimajiri, *Bioelectrochem. Bioenerg.,* **47** (1998) 333-342

Aggregation effects in cell suspensions
RBC in blood plasma vs. RBC in PBS

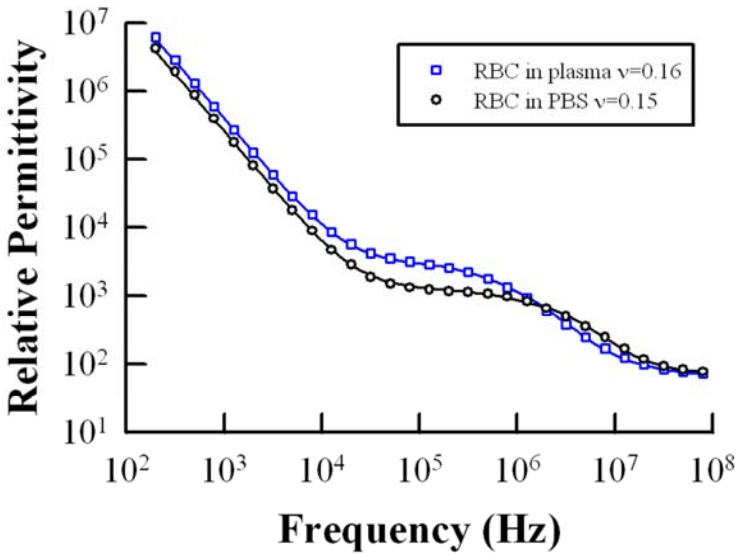

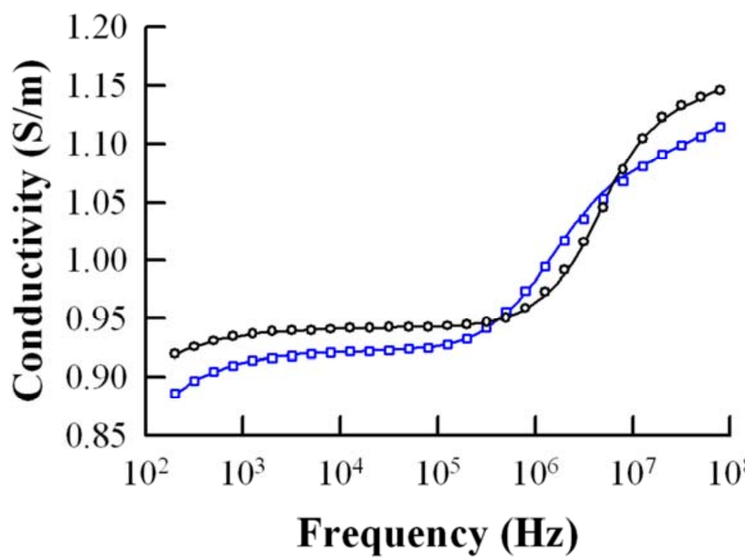

RBC in plasma forms reversible structures (rouleaux), through fibrinogen-mediated bridging, even at low concentrations → aggregation effects can be separated from concentration effects using RBC.

Photo obtained from:
http://bloodjournal.hematologylibrary.org/cgi/content/full/107/11/4205

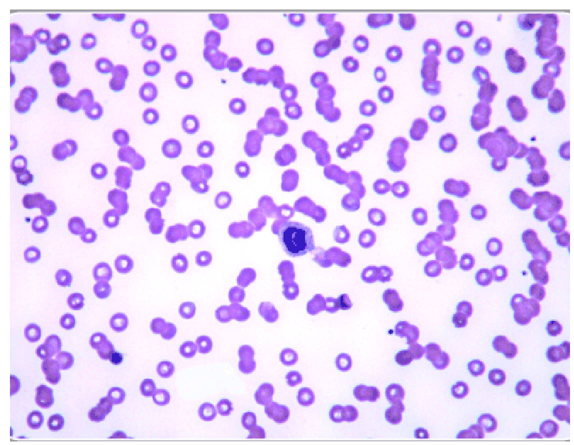

Normal vs. abnormal tissue structure

Detection of breast cancer

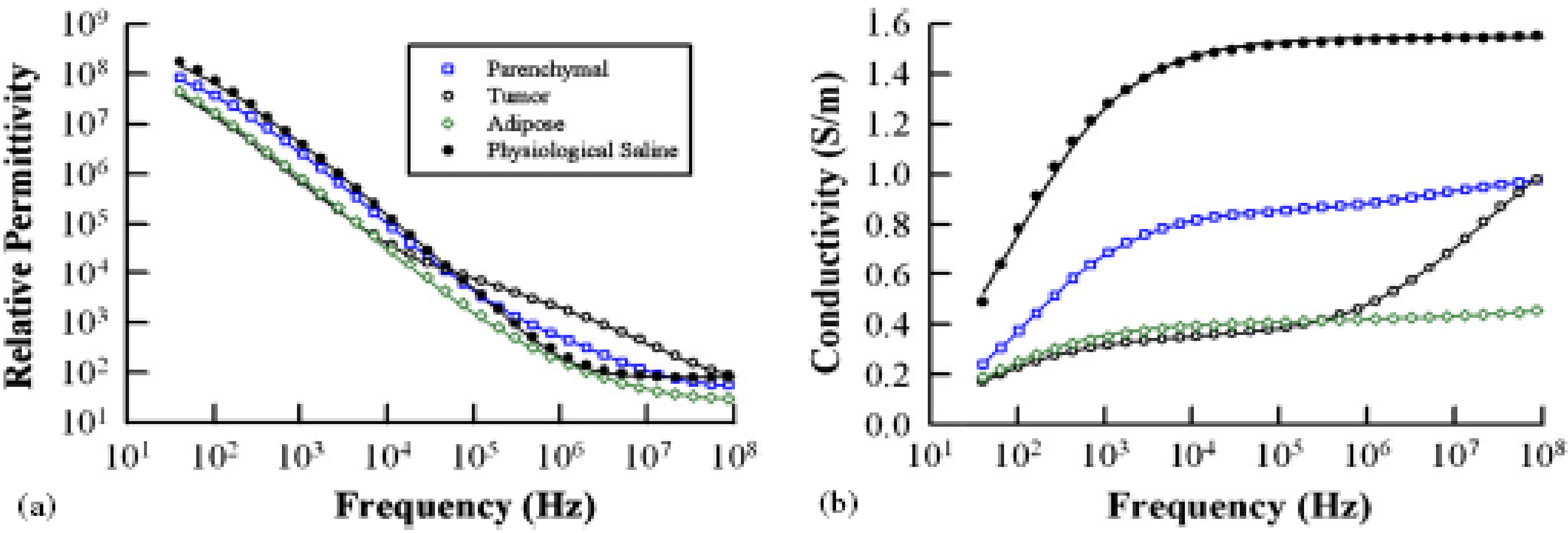

Since dielectric spectroscopy is sensitive to supra-cellular architecture, it can be used to distinguish normal from cancerous tissues

M. R. Stoneman, M. Kosempa, W. D. Gregory, C. W. Gregory, J. J. Marx, W. Mikkelson, J. Tjoe, and V. Raicu, 2007, *Phys. Med. Biol.,* **52:** 6589-6604

Normal vs. abnormal tissue structure

1-D scanning of breast tumor

Table 3. Best-fit parameters for the dielectric data obtained using the probe-scanning protocol described in section 4.3 for a breast tissue containing a tumor. The value of $\eta = 0.45$ was determined from physiological saline measurements carried out directly prior to tissue measurements. Fitting residual was calculated in accordance with equation (8).

Distance from 'zero' point (mm)	Δ	f_c (MHz)	α	β	ε_h	σ_I (S m^{-1})	K	Fitting residual
0.0	350	13.6	0.430	0.079	59.2	0.764	8.71	4.19
7.0	600	3.72	0.361	0.172	63.0	0.892	10.30	2.50
14.0	3800	2.40	0.322	0.110	50.2	0.150	4.16	3.29
15.0	3700	2.13	0.340	0.136	45.6	0.131	0.03	4.00
17.5	2200	4.41	0.364	0.115	47.2	0.212	4.17	3.34
21.5	2700	2.62	0.328	0.130	54.2	0.469	6.22	2.79

This preliminary study constitutes a primitive form of (one-dimensional) imaging.

M. R. Stoneman, M. Kosempa, W. D. Gregory, C. W. Gregory, J. J. Marx, W. Mikkelson, J. Tjoe, and V. Raicu, 2007, *Phys. Med. Biol.*, **52**: 6589-6604

2-D imaging using dielectric spectroscopy

The ‘travelling’ coaxial probe

→ A coaxial probe, created from an array of planar electrodes, is scanned across the sample using electronic switches.

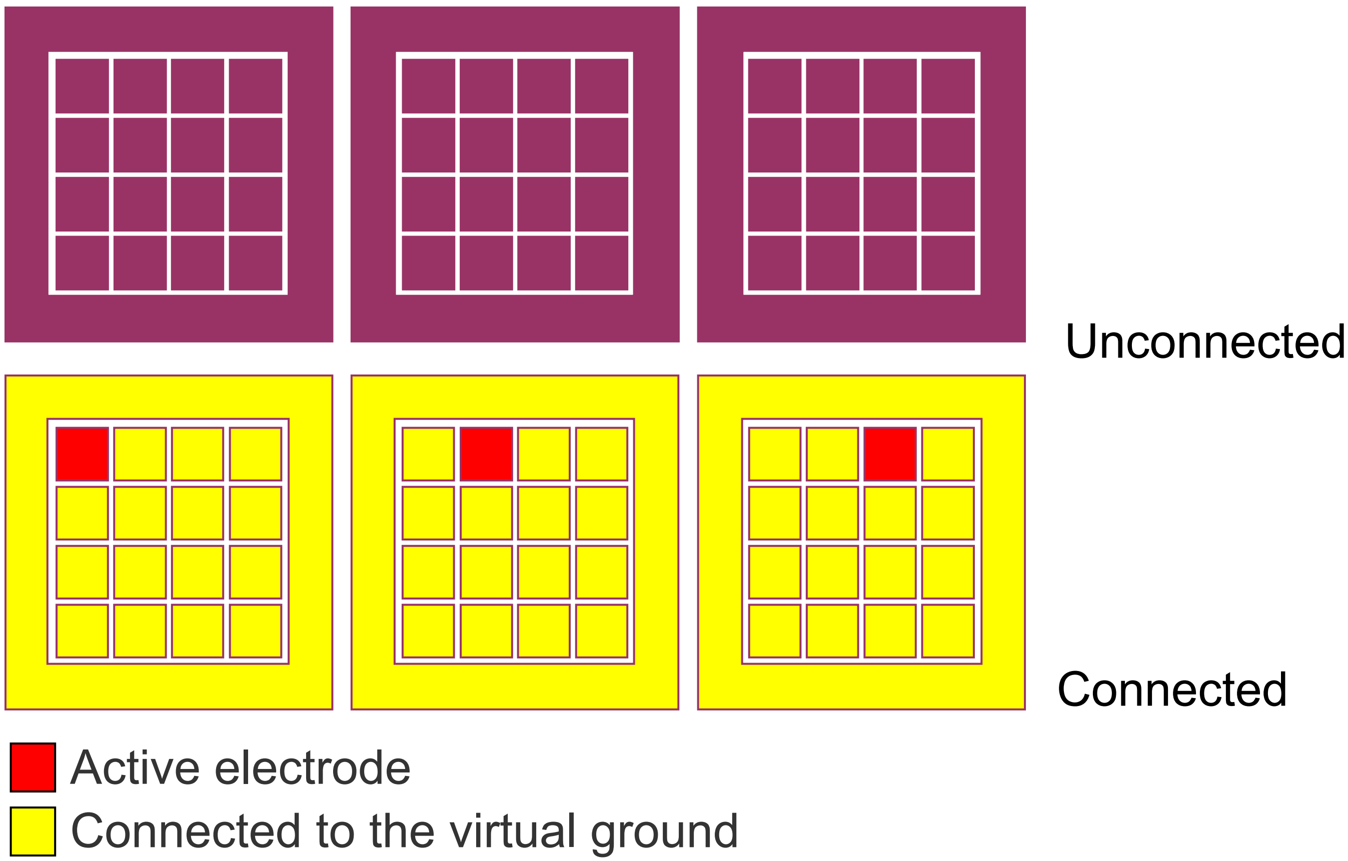

M. Habibi, D. Klemer, V. Raicu, *EMBC Conference Proceedings*, 2009, in press

2-D imaging using dielectric spectroscopy

Dielectric measurements of a tissue phantom

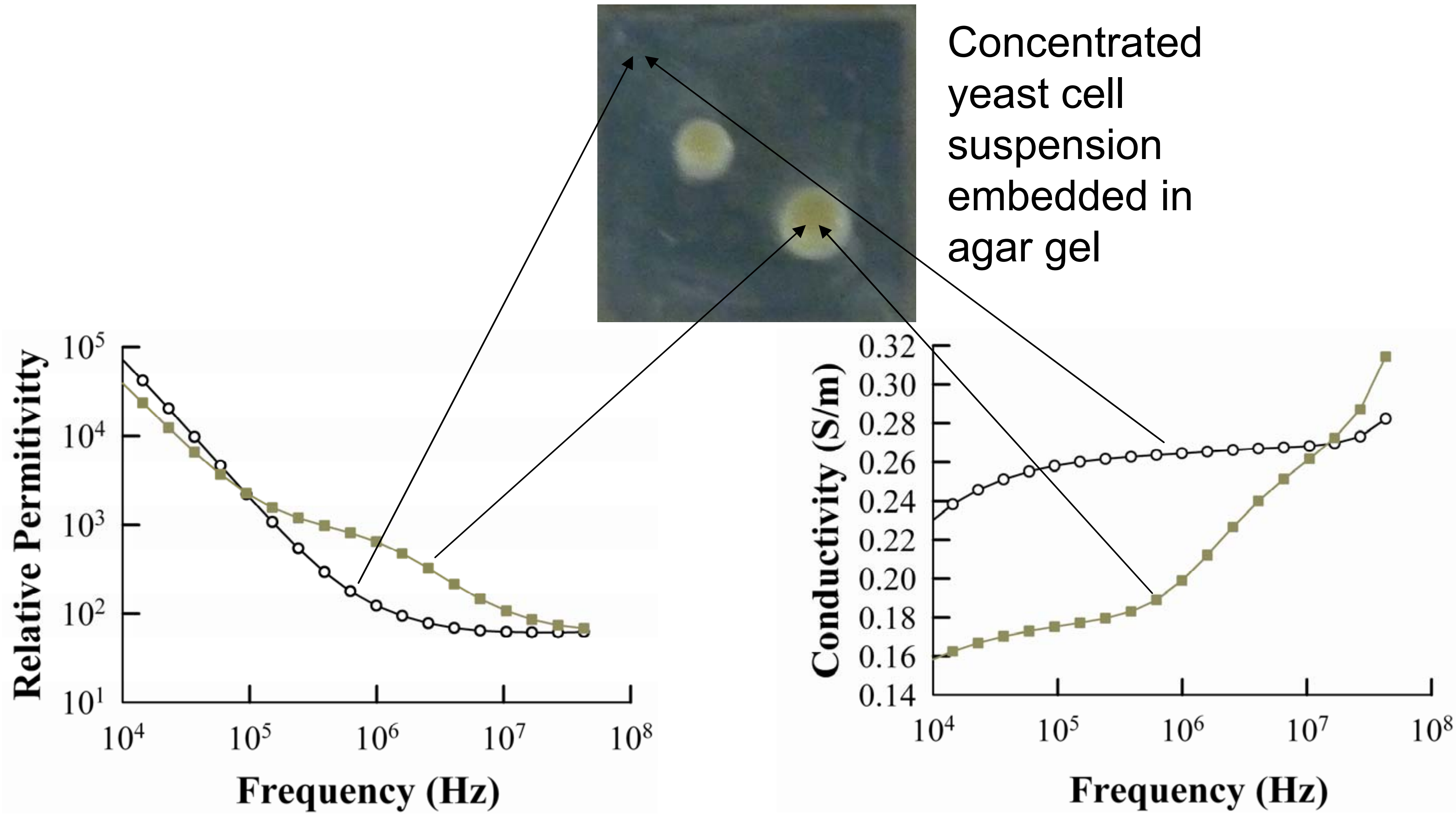

M. Habibi, D. Klemer, V. Raicu, *to be submitted,* 2009

2-D imaging using dielectric spectroscopy

Spatial mapping of the tissue phantom

Digital photograph

Low-frequency (σ_l) conductivity map

S/m

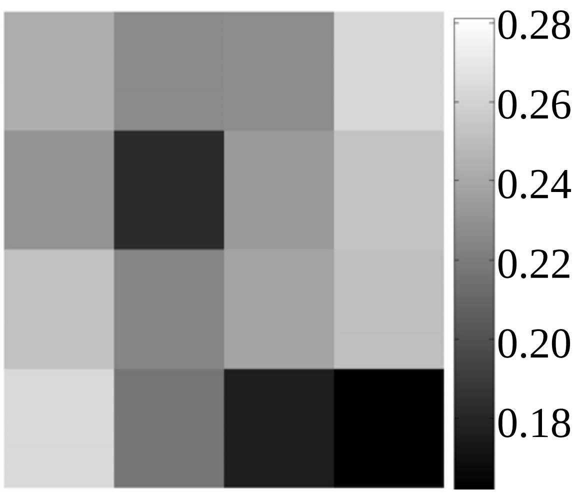

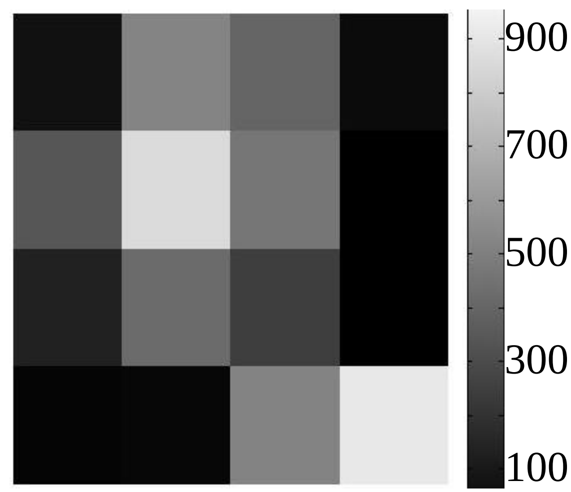

Dielectric increment map

M. Habibi, D. Klemer, and V. Raicu, *to be submitted,* 2009

Dielectric dispersion of rat brain in vivo

- Dielectric dispersion of brain was best represented by a sum between a Cole-Cole and a Debye dispersion function
- In addition, neurons and astrocytes in brain are connected not only by chemical synapses, but also by electrical synapses, which are also known as **gap-junctions**

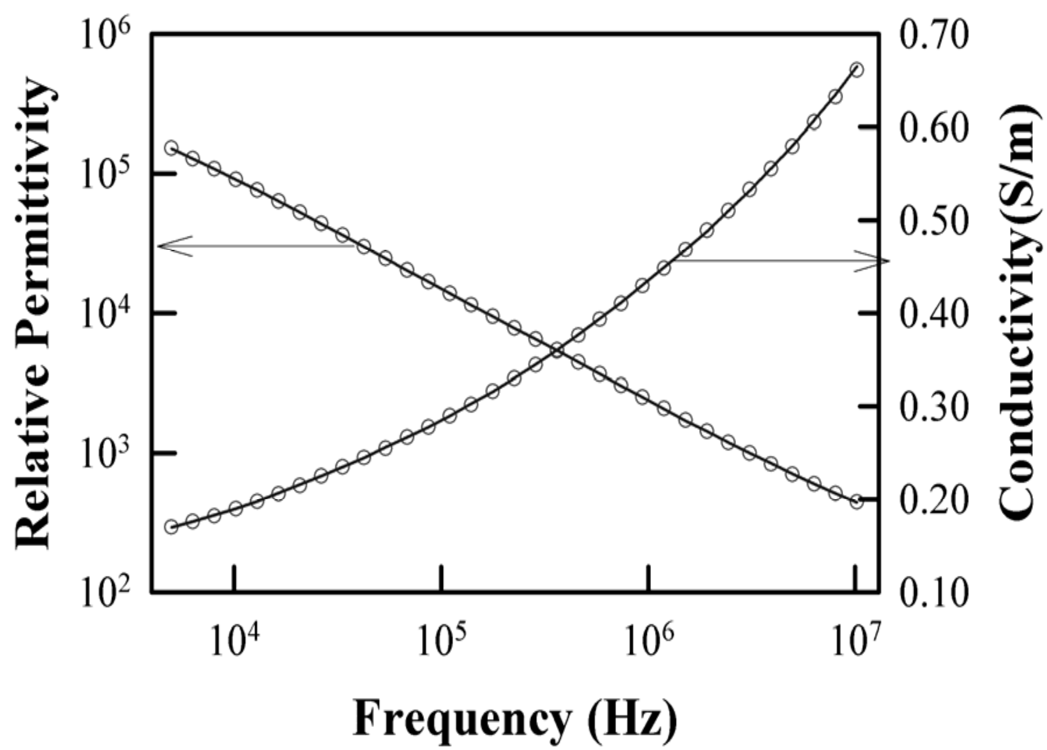

M. Florescu, V. Sahore, M. Stoneman, et al., *to be submitted*, 2009

Anesthetic effects on gap-junctions in brain

We treated rats with:

➢ an anesthetic (Isoflurane) known to act as a gap-junction blocker (i.e., to disconnect cells from one-another)

➢ a non-anesthetic (CBX) that acts as a gap-junction blocker

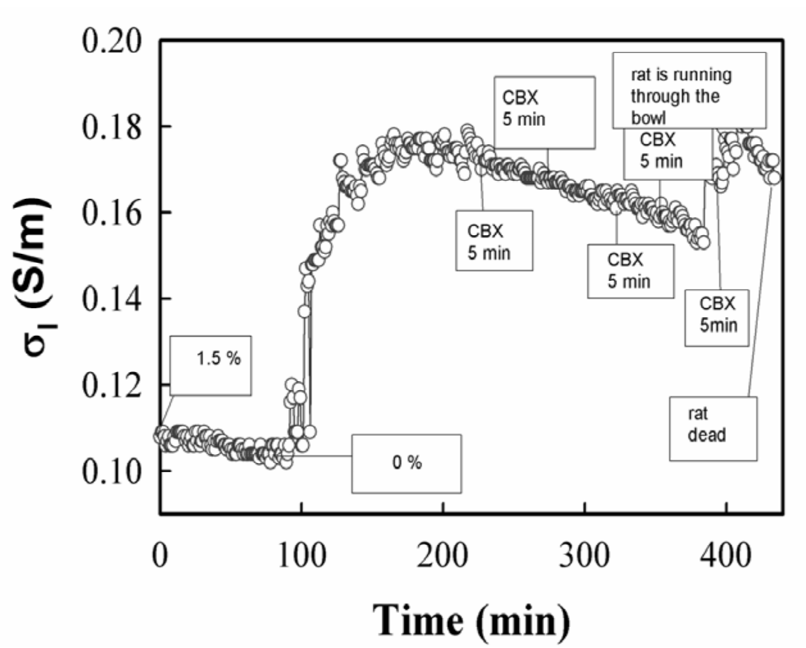

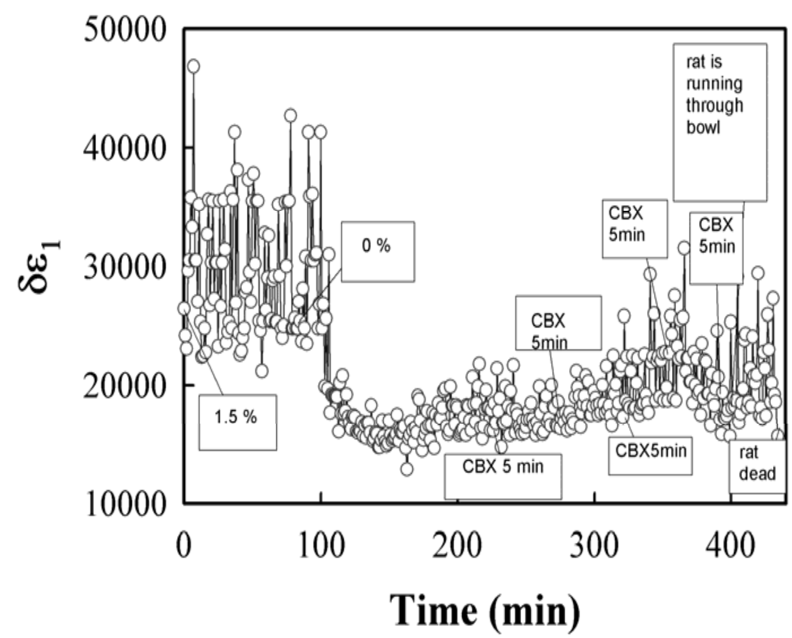

M. Florescu, V. Sahore, M. Stoneman, et al., *to be submitted*, 2009

Summary and outlook

Dielectric spectroscopy may be used to determine intrinsic electrical parameters of cells in dilute suspensions.

The supra-cellular architecture in tissues causes non-Debye dielectric behavior, which can be used to:

- Image inhomogeneities in tissues
- Detect structural differences between normal and cancerous tissues
- Monitor changes in brain function by detecting changes in the inter-cellular connectivity between neurons

Novel theories are needed for tissues, to incorporate:

- High cellular concentrations (EMT)
- Cell aggregation (e.g., using EMT-DDI or higher order corrections)
- Percolative structures (i.e., clusters are connected with other clusters)
- Coupling between cytoplasms through gap-junctions

Acknowledgements

Research group members

Monica Florescu, postdoctoral research associate
Michael Stoneman, graduate student, physics
Mohammad Habibi, graduate student, electrical engineering
Vishal Sahore, graduate student
Deo Raj Singh, graduate student, physics
Rinki Singh, graduate student, physics
Michael Roesch, undergraduate student, biochemistry

Collaborators

Prof. Anthony Hudetz, Medical College of Wisconsin
Prof. William Gregory, University of Wisconsin, Milwaukee
Prof. David Klemer, University of Wisconsin, Milwaukee
Numerous others, who contributed over the past two decades